Friction

Research Article

Study on wear performance and mechanism of pantograph contact strip that contact with damaged contact wire under ambient humidity

Xingshuai Zhi[1], Ning Zhou[1,✉], Yao Cheng[1], Haifei Wei[1], Yongming Yao[2], Weihua Zhang[1], Guangxiong Chen[3]

Cite this article: Zhi XS, Zhou N, Cheng Y, et al. *Friction* 2026, **14**(2): 9441101. https://doi.org/10.26599/FRICT.2025.9441101

ABSTRACT: Studies have focused on the significant impact of contact wire damage on the abnormal wear of pantograph contact strips. Initially, on the basis of field data analysis, the most common types of contact wire damage were identified. The experiments and wear performance analysis of contact strips in contact with damaged contact wires were subsequently conducted at high and low humidities. Finally, correlation analysis was employed to explore the influence of various factors on strip wear performance. The results indicate that excessive wear occurs on the contact strip with the pitted contact (PC) wire, particularly under low humidity, where the strip wear rate is 2.2 times greater than that of the contact strip with the normal contact (NC) wire. While in contact with a PC, the primary wear mechanisms of the contact strip include material transfer and arcing ablation under high humidity but involve material transfer, arcing ablation, and microcutting under low humidity. Correlation analysis revealed that under low humidity, the parameters related to PC had the greatest impact on the wear rate of the contact strips, with a significant increase in the mechanical wear proportion. On the basis of these findings, both contact wire damage and reduced humidity contribute to more severe abnormal wear of the contact strip, with the influence of PC conditions being more excessive than that of reduced humidity on wear performance.

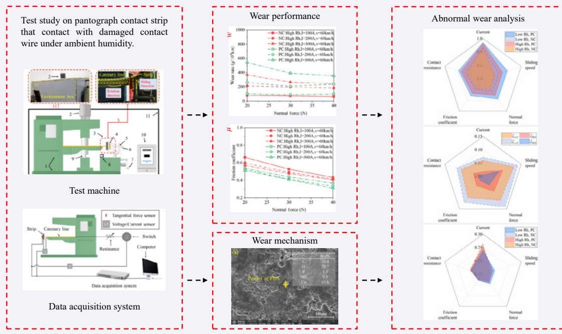

KEYWORDS: pantograph–catenary system; contact strip; abnormal wear; wear mechanism; ambient humidity

1 Introduction

The pantograph and catenary system (PCS) is the only means of energy collection for electrified trains and is one of the key subsystems for ensuring safe and stable train operations. In contemporary electrified railway systems, the primary structures of the train current collection include an overhead flexible catenary, a rigid catenary, and contact rails. The rigid catenary has become the preferred choice for urban rail trains because of its economic benefits and operational conditions [1]. The pantograph is mounted on the roof of the train, and the contact wire is arranged in a sinusoidal pattern along the centerline of the track to prevent continuous wear at a certain point on the contact strip. The pantograph, under the lift of vertical forces, collects the current transmitted through the contact strip by sliding contact with the contact wire, as illustrated in Fig. 1. The dynamic interaction of the PCS is highly complex with high relative sliding speeds, resulting in excessive wear of the contact surface, which greatly increases the operational and maintenance costs as well as the risks associated with train operations. Therefore, research on the evolution of contact pair wear performance and its impact on the dynamic interaction of the PCS after contact wire damage has become urgent.

The wear performance of contact pairs is influenced not only by their intrinsic properties but also by the tribological system and its specific structure and wear mechanisms [2–4]. The contact pair of the PCS operates under high sliding speeds and excessive current densities over extended periods, resulting in numerous factors affecting wear performance; notably, as previously mentioned, the tribological system and its specific structure have a more pronounced impact. According to current research, the influencing factors can be categorized into four main types: system structure and materials, service environment, contact interface characteristics, and operating parameters. A critical aspect concerns the structure and materials of the PCS, which includes the material properties of the contact pair [5–9], the stiffness and

[1] State Key Laboratory of Traction Power, Southwest Jiaotong University, Chengdu 610031, China. [2] Infrastructure Inspection Research Institute, China Academy of Railway Sciences Corporation Limited, Beijing 100081, China. [3] Tribology Research Institute, School of Mechanical Engineering, Southwest Jiaotong University, Chengdu 610031, China.

✉ Corresponding author. E-mail: zhou_ningbb@sina.com

Received: December 3, 2024; Revised: February 13, 2025; Accepted: March 18, 2025

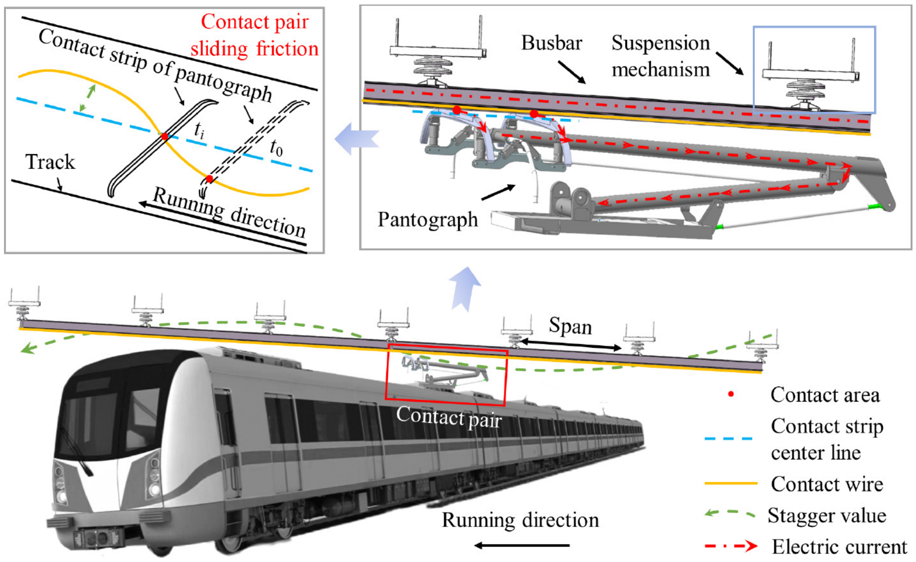

Fig. 1 Sliding friction and current collection diagram of PCS contact pair.

mass of the components [10], the length and diameter of the rods [11], the unevenness of the contact wire [12], and the arrangement of the contact wire stagger values [13, 14]. Ongoing field monitoring and in-depth research have gradually revealed the influence of humidity, given the complex and variable railway environment encountered during train operations, such as sudden adverse weather, altitude pressure variations, and fluctuations in environmental temperature and humidity [15–18]. In research addressing the sliding friction behavior of contact pairs under various humidity levels, Moberly and Johnson [19] conducted targeted experiments on carbon brushes, identifying the critical humidity level that leads to catastrophic wear of the brushes. Building on this, Hu et al. [20] performed tests under conditions of both high and low humidity relative to this critical humidity and discussed the reasons for excessive wear of the carbon brushes, attributing it to the difficulty in forming a cuprous oxide protective film under low humidity conditions. Furthermore, ongoing research has also demonstrated that environmental humidity significantly affects the contact resistance, friction coefficient, arcing energy, and even the wear mechanism [21, 22]. This leads to contact surface damage and affects the dynamic and tribological properties of the material, which causes abnormal contact pair wear [23]. Therefore, to address the issue of changes in the contact state, Ren et al. [24] investigated the wear performance of contact pairs under different damage forms, namely, normal, pitted, and oblique contact wires. The results showed that the oblique contact wire results in the most severe deterioration in wear performance due to increased electrical wear. On the other hand, understanding the evolution of the wear performance of the contact pair under different operational parameters is crucial, as it directly impacts maintenance and parameter adjustments. These adjustments include variations in the operating speed [25–27] and static normal force [28–33], which affect both electrical and mechanical wear [1].

Through the aforementioned investigations and prior research analyses, a significant correlation between environmental humidity and the occurrence of abnormal wear was found, and detailed experiments and discussions were conducted. However, current studies rarely associate abnormal wear with ambient humidity. Furthermore, the experimental conditions do not sufficiently replicate actual operational scenarios. For example, there can be a discrepancy of 5–10 times in sliding speed and hundreds of times in current density, which is likely to lead to deviations in wear mechanisms from those observed under actual conditions. Additionally, the effect of actual contact pair damage on wear performance appears to have been insufficiently studied, highlighting a critical direction in this research. In previous studies, the causes of PCS contact pair abnormal wear were preliminarily investigated, particularly concerning ambient humidity. It was confirmed that humidity significantly impacts the wear rate and leads to variations in parameters such as the friction coefficient and contact resistance, which damage the surface profile of the contact strip and contact wire [20–23]. Given that it is impractical to repair the contact wire after every operation in actual maintenance and to quantify the differences in the wear performance of strips before and after damage under varying environmental humidities, a series of experiments and correlation analyses were carried out, which will enhance the understanding of the wear mechanisms and abnormal wear evolution laws of PCS contact pairs. Ultimately, this research provides valuable insights into the causes of abnormal wear in the PCS and serves as a theoretical basis for improving the wear performance and dynamic interaction.

The remainder of this paper is organized as follows. In Section 2, a data tracking analysis was conducted, revealing a significant correlation between abnormal PCS wear, environmental humidity, and contact wire damage, and an experimental scheme was carried out. In Section 3, a series of experiments were conducted to replicate contact wire damage under both high- and low-humidity conditions. Additionally, an analysis of the performance evolution law and wear mechanisms was performed. In Section 4, a relational analysis was conducted to assess the factors influencing wear performance, comparing the effects of different humidities and damaged contact wires. Section 5 integrates the findings from the previous sections to further elucidate the causes of abnormal wear. Finally, the main conclusions are summarized in Section 6.

2 Field tests of the contact wire and test preparations

This section discusses the long-term tracking results of the wear rate on the contact strip of the pantograph, focusing on the relationship between the wear rate and environmental humidity/contact wire damage. It also provides a statistical analysis of the types and percentages of damaged contact wires observed during

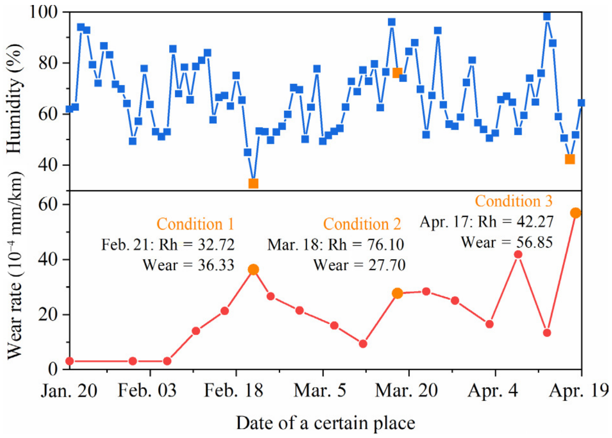

Fig. 2 Tracking results of humidity and strip wear rate.

this period, as well as the design of the experimental conditions, which serve as the foundation for this study.

2.1 Field tests of the contact wire and contact strip wear rates

In the past several years of continuous monitoring, a significant inflection point was observed when the environmental humidity decreased, leading to a sharp increase in the wear rate of the strip, as illustrated in Condition 1 of Fig. 2. However, high strip wear rates were also noted under conditions of elevated humidity, as shown in Condition 2 of Fig. 2. To further investigate these phenomena, detailed tracking and surveys of actual field conditions were conducted. Figure 3 presents the macroscopic surface of the contact wire (counterbody of the strip), which can be categorized into five types on the basis of the observed conditions. Types A–D represent four categories of damage, whereas Type E indicates a contact surface with a well-formed smooth oxide layer. Following the occurrence of Condition 2, a sampling statistical analysis was performed on the field contact wire surface across several abnormal wear sections (approximately 240 m), as shown in Fig. 4, where a high percentage of severe surface damage to the contact wire was evident. This suggests that the abnormal wear observed in Condition 1 likely deteriorated the contact wire surface, leading to significant impacts on the strip wear rate once the damage accumulated beyond a certain threshold, triggering Condition 2. Furthermore, following this situation, further damage to the contact wire surface occurred because of inadequate maintenance. As the environmental humidity continued to decrease, the wear rate of the strip increased to catastrophic levels, leading to the emergence of Condition 3. Therefore, further research is urgently needed.

2.2 Test preparations and methods

The test uses a pantograph–catenary contact pair friction and wear testing machine. Figures 5(a) and 5(b) show the schematic diagram and data acquisition system of the machine, respectively. To maintain stable environmental humidity, an external environmental control room was added to the test machine, and an industrial-grade dehumidifier was used to control the humidity levels. An investigation and analysis of the wear performance of subway lines in multiple locations revealed that the wear rate

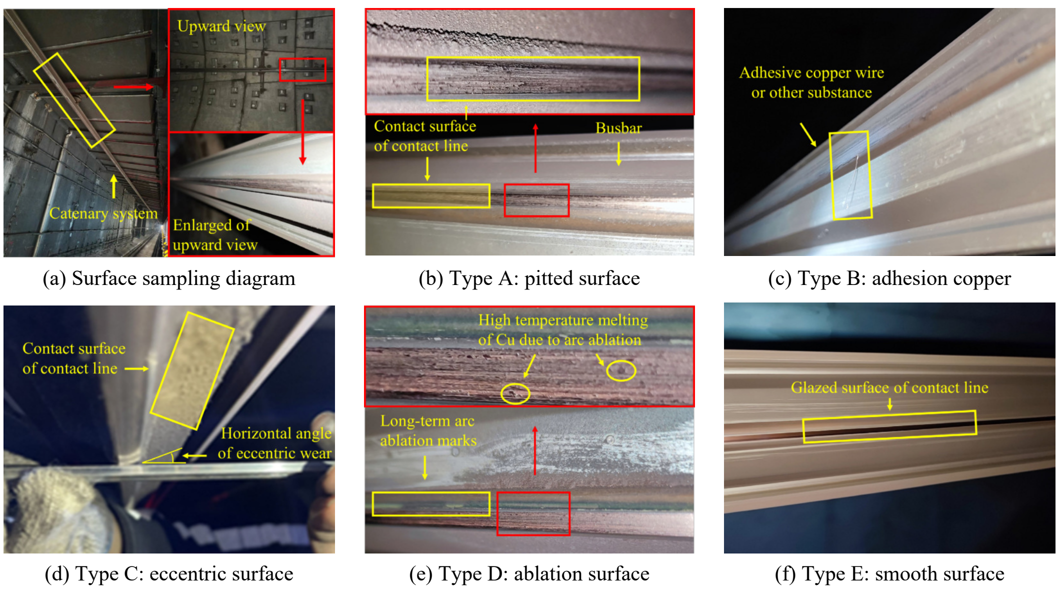

Fig. 3 Types of contact wire surface damage.

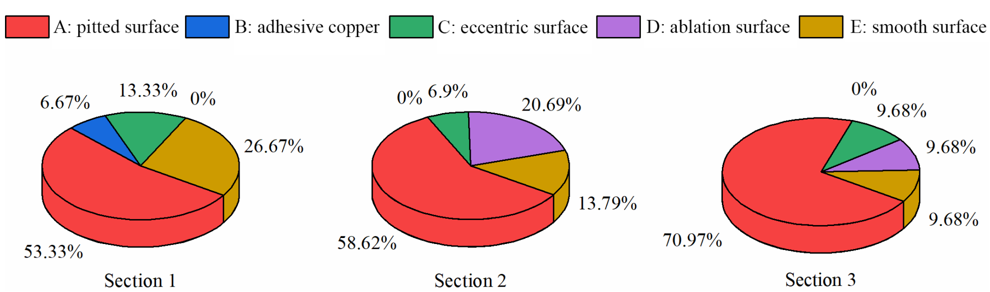

Fig. 4 Quantity percentage of contact wire surface damage.

清華大学出版社 Tsinghua University Press | SciOpen

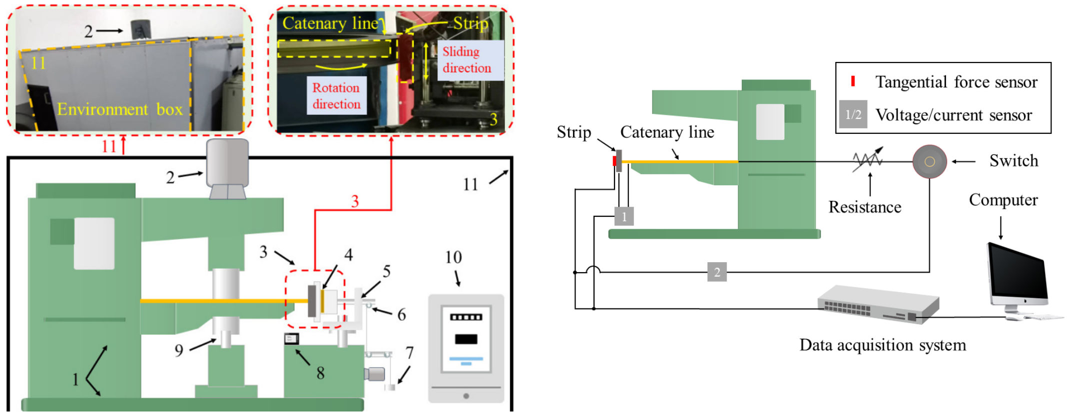

(a) Test machine (b) Data acquisition system

Fig. 5 (a) Test machine and (b) data acquisition system. Note: 1. test machine construction frame, 2. variable-frequency motor, 3. contact pairs, 4. insulator, 5. vertical reciprocating frame, 6. pulley, 7. normal force loading device 8. temperature and humidity detector, 9. mercury, 10. industrial grade dehumidifier, and 11. environmental room.

increases sharply when the humidity drops below 30%. Therefore, the humidity was maintained at 20%–25% for low humidity and 50%–55% for high humidity (to simulate the actual situation) during the tests. The wear volume of the strip is determined by measuring the mass difference before and after the wear process via a balance with an accuracy of 0.001 g. The wear rate is defined as the wear volume divided by the sliding distance. In the experiment, Hall sensors are used to measure the voltage and current. The friction coefficient, current, and voltage are collected by the data acquisition system and stored in the computer system, with a sampling rate of 1,000 Hz. The specific parameters of the test machine can be found in Ref. [23].

According to Fig. 4, the contact wires of Type A exhibit the highest proportion of damaged contact wires. Therefore, experiments were conducted using Type A contact wires with pitted (PC) and normal contact (NC) wires under different humidity conditions. The surfaces of the contact wires used in the experiments are illustrated in Fig. 6. For the NC, each experiment involved sanding the contact wires both longitudinally and transversely (relative to the direction of rotation) with 800# and 1500# sandpaper in sequential order. After each sanding, the surfaces were rinsed and wiped with 95% alcohol to remove any residual debris or foreign particles. For the PC, actual damaged contact wires (Type A, as shown in Fig. 3) were embedded into the test machine. The experimental conditions were designed to closely simulate actual operational scenarios, with parameters set to a current of 0–300 A, a normal force of 20–40 N, and a sliding speed of 60–80 km/h, as detailed in Table 1.

The experiments utilized Cu-Ag alloy contact wires and metal-impregnated carbon strip samples measuring 135 mm × 30 mm × 24 mm as the friction pair, both of which are materials employed in actual railway operations. The elemental compositions of the samples are presented in Tables 2 and 3.

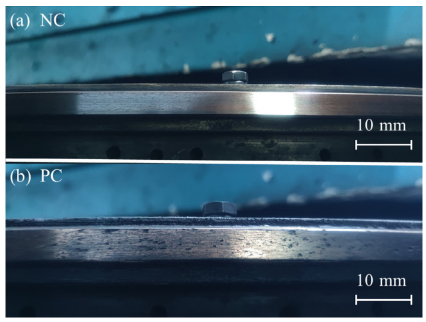

Fig. 6 Contact wire surface state of test machine.

Table 1 Test conditions under high and low humidities

Current (A)	0, 100, 200, and 300				
Normal force (N)	20		30		40
Sliding speed (km/h)	60	60	70	80	60

Table 2 Chemical composition of the contact wire

Component part	Weight (%)
Cu	Everything else
Ag	0.08–0.12
Bi	⩽ 0.0005
O	⩽ 0.003
Others	⩽ 0.03

Table 3 Chemical composition of the strips

Component part	Weight (%)
C	88.3
Cu	11.4
Others	⩽ 0.3

3 Wear tests of strips that contact damaged contact wires under different humidities

To investigate the effects of parameters such as current, sliding speed, and normal force on the wear evolution law of contact strips that contact damaged contact wires, multiple sets of wear experiments were conducted, considering the influence of humidity. This section primarily compares the effects of PC and NC on strip wear performance, as well as the effects of humidity, which are discussed in two separate subsections. These findings provide valuable insights for operational and maintenance guidance. Additionally, the differences in the microstructures of the strips in contact with PC and NC, as well as the variations in the microstructures under high- and low-humidity conditions in contact with PC, were compared.

3.1 Experimental results of the wear tests

3.1.1 *Evolution law of the wear rate under different humidities*

The damaged contact wire observed in the field is likely to cause more excessive wear on the strip. The experimental results addressing this issue are presented in Fig. 7, facilitating a better understanding of the wear evolution law.

Figures 7(a)–7(c) show the contact strip wear rates under high humidity with NC and PC as the counterbody, respectively. Under identical operating parameters, the wear rate in contact with the PC significantly exceeds that in contact with the NC, with the wear rate ranging from approximately 1.2 to 1.6, and the absolute difference reached a maximum increase of 174.25×10^{-4} g/km. Additionally, the wear rate for both conditions increases rapidly with increasing current due to the Joule heating effect and tends to increase with increasing sliding speed, which is attributable to the increase in mechanical and electrical wear caused by vibration. Notably, the wear behavior slightly differed in response to changes in the normal force between the two conditions. In contact with NC, the wear rate decreases with normal force due to the reduced proportion of electrical wear. Conversely, when the current is 100 and 200 A, a critical point is observed at a normal force of 30 N, where the wear rate first decreases and then increases with the normal force. Previous studies have indicated that the wear performance of contact strips is influenced primarily by electrical and mechanical wear. At lower normal forces, electrical wear dominates, leading to a decrease in the wear rate with increasing force. However, as the normal force continues to rise, a positive correlation between the wear rate and normal force emerges, driven by the predominance of mechanical wear [28–31]. In this study, the increased surface roughness of the PC contact wire increased the degree of mechanical wear of the strip. Consequently, a lower normal force is sufficient to reach the wear rate critical threshold. Thus, the wear rate initially decreases and then increases with increasing normal force. Ref. [31] has examined the critical threshold of wear rate changes with normal force under varying conditions, highlighting the competitive relationship between mechanical and electrical wear at different operating parameters. As the current increases, this critical threshold gradually increases, which explains why, at 300 A, the wear rate still decreases with increasing normal force. Figures 7(d)–7(f) present the contact strip wear rates under low humidity with NC and PC as counterbodies, respectively. Similar to a high-humidity environment, it is evident that the wear rate in contact with PC significantly exceeds that in contact with NC under identical operating parameters. However, the relationship between the wear rate and normal force exhibits a critical threshold only when the current is 100 A, specifically between 20 and 40 N, which is attributed to the increased proportion of electrical wear resulting from the PC condition.

Figure 8 shows the contact strip wear rate under various humidity levels. This comparison facilitates an analysis of how damage to the contact wire influences the wear performance of strips under different humidity conditions.

Figures 8(a)–8(f) show the contact strip wear rates with NC and PC as counterbodies under low and high humidities, respectively. Under identical operating parameters, the wear rate under low humidity clearly significantly exceeds that under high humidity, with the wear rate increasing by a maximum of approximately 2.2 times and the absolute difference reaching a maximum increase of 181.5×10^{-4} g/km, which is particularly pronounced at higher currents, leading to significant wear at the contact interface.

3.1.2 Evolution law of the friction coefficient under different humidities

The friction coefficient (μ) of the contact pairs of the contact interface primarily depends on the deformation components of the microcontact interacting at the contact surfaces (plowing deformation) and the adhesion components between the adhesion of the microcontact [3, 34]. In this study, the proportions of these two components further contribute to several variations due to damage to the contact wire, resulting in differences in μ, as illustrated in Fig. 9.

Figures 9(a)–9(c) illustrate the evolution law of μ under high humidity with NC and PC as the counterbody, respectively. Under identical operating parameters, the μ that contacts the PC

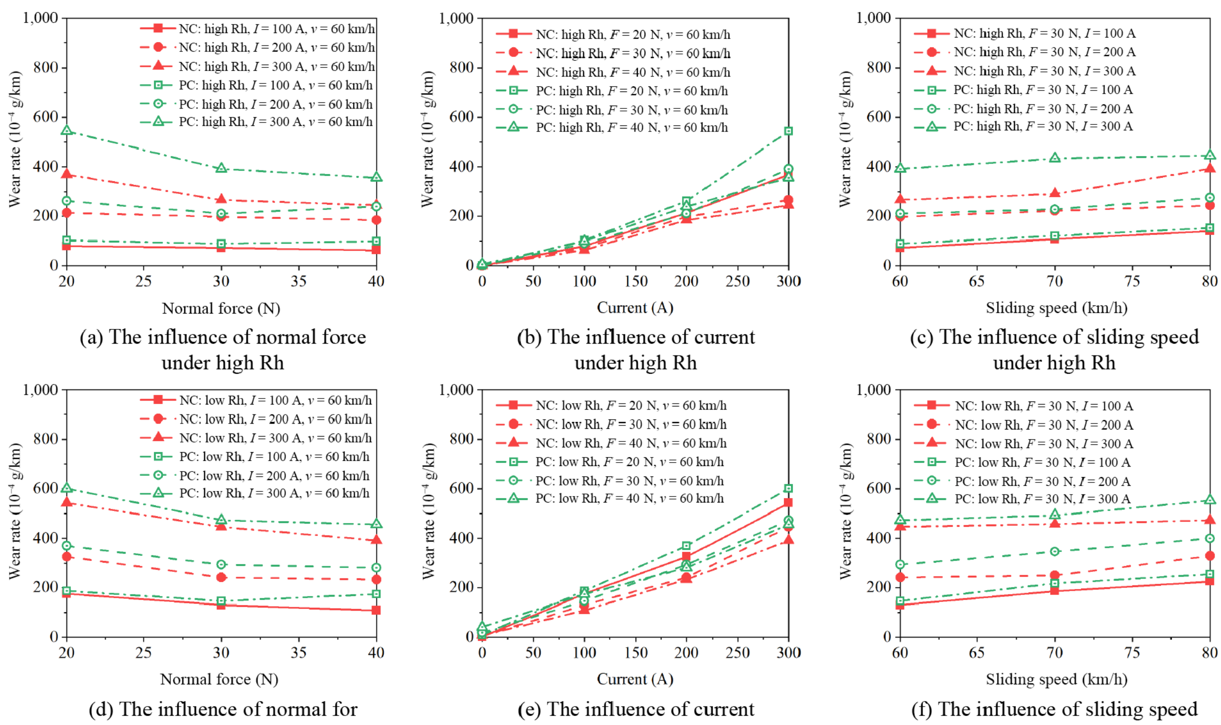

(a) The influence of normal force under high Rh

(b) The influence of current under high Rh

(c) The influence of sliding speed under high Rh

(d) The influence of normal for ceunder low Rh

(e) The influence of current under low Rh

(f) The influence of sliding speed under low Rh

Fig. 7 Evolution law of wear rate under different humidities.

清華大学出版社 Tsinghua University Press | SciOpen

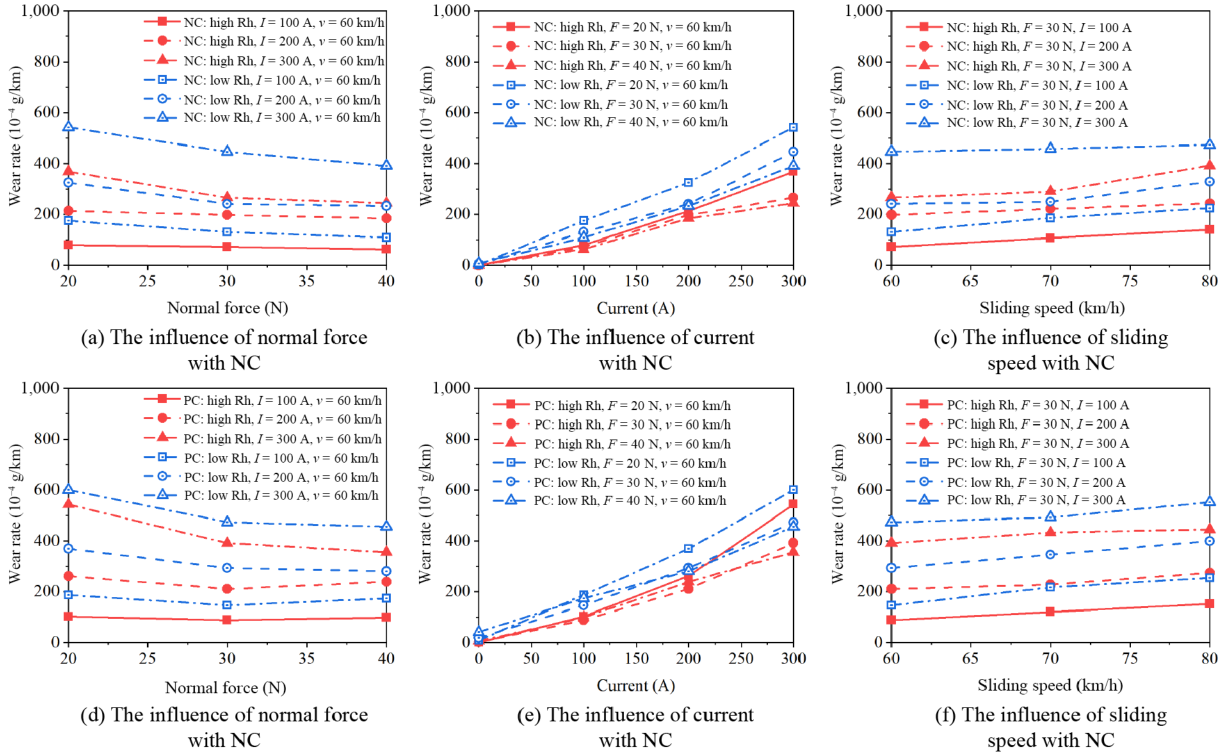

(a) The influence of normal force with NC
(b) The influence of current with NC
(c) The influence of sliding speed with NC
(d) The influence of normal force with NC
(e) The influence of current with NC
(f) The influence of sliding speed with NC

Fig. 8 Evolution law of the wear rate with different counterbodies.

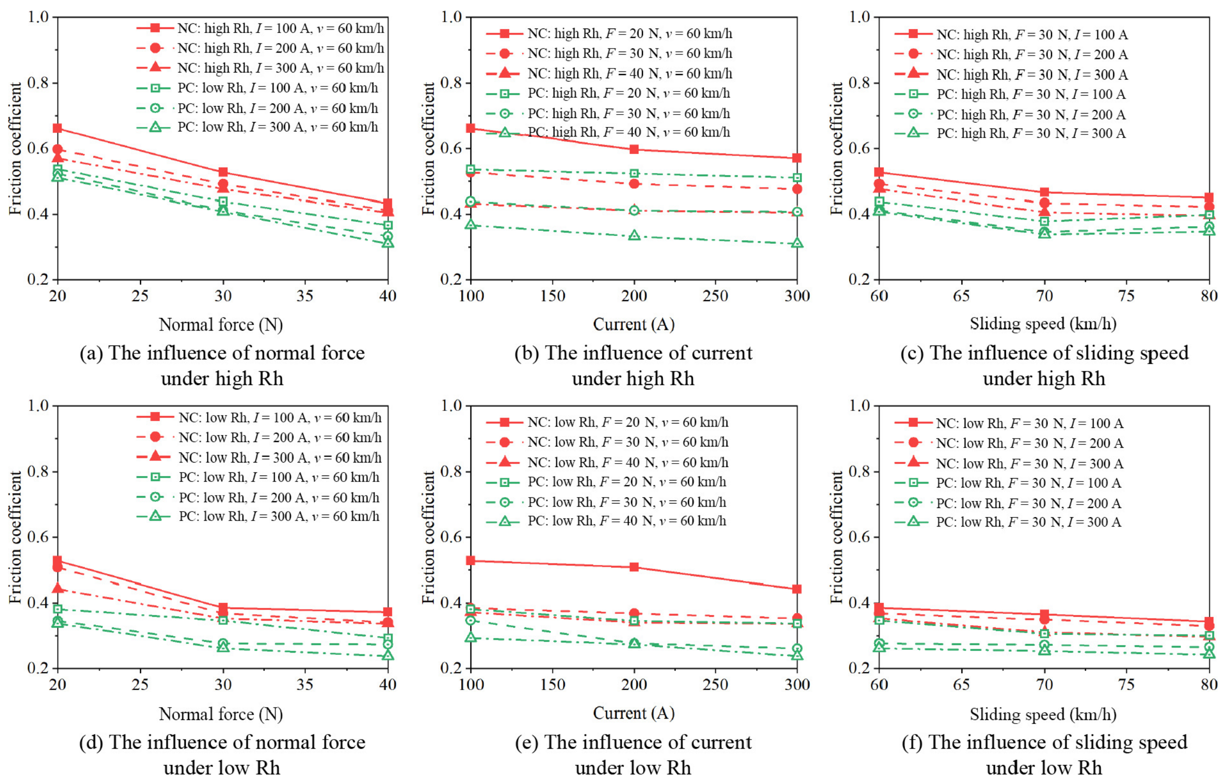

(a) The influence of normal force under high Rh
(b) The influence of current under high Rh
(c) The influence of sliding speed under high Rh
(d) The influence of normal force under low Rh
(e) The influence of current under low Rh
(f) The influence of sliding speed under low Rh

Fig. 9 Evolution law of μ with different counterbodies.

is consistently lower than that that contacts the NC. Furthermore, μ, which is in contact with the NC and PC, tends to decrease with increasing normal force, current, and sliding speed, regardless of the humidity level.

The process by which contact strips collect current from contact wires is characterized as sliding electrical contact under high electrical load contact, which is often accompanied by mechanical, thermal, and electrical effects (including electric sparks and arcing). As the normal force increases, the actual contact area between the contact pair surfaces also increases [35, 36]. Furthermore, the microbulges on the rough surface penetrate the oxide film and other contaminant film, resulting in an increased metallic contact area and conductive contact area, which leads to a reduction in contact resistance and arcing. In this process, the adhesion component of the friction process is significantly dominant. However, as the normal load increases, the contact behavior of the rough microbulge peaks transitions from elastic to elastoplastic and ultimately to plastic deformation, which reduces the adhesion component and decreases μ. A comparison between the performance contact with NC and PC, regardless of humidity levels (Figs. 9(a)–9(f)), reveals that the PC contact surfaces are rougher, with larger peak heights and smaller radii of curvature at the peaks, resulting in a reduction in the adhesion component, as to decrease μ. Additionally, owing to the roughness of the PC surface, the arcing energy is greater [24], leading to a significant temperature rise in the contact pair, which further provides a lubricating effect that results in μ being lower than that in contact with NC under equivalent conditions. Moreover, the temperature of the contact pair can vary to different extents due to the increase in sliding speed and load current, which creates a complex mapping relationship between μ and the operational parameters. On the one hand, as the current and operating speed increase, the temperature rise in the contact pair softens the material, reducing the adhesion component of friction and leading to a decrease in μ. On the other hand, the increase in temperature enhances the lubrication effect of the graphite particles within the strip and promotes the formation of an oxide film within the contact pair, further contributing to the reduction in μ.

Figures 10(a)–10(f) illustrate the evolution law of the μ contact with the NC and PC as counterbodies under low and high humidities, respectively. Under identical operational parameters, μ under low-humidity conditions is consistently lower than that under high-humidity conditions, which aligns with previous research results [16, 22, 23]. However, under noncurrent conditions, μ is lower at high humidity because of water film formation, and the significant temperature rise in the contact pair under excessive current conditions renders the influence of the water film negligible. The greater contact pair temperature increase under low humidity leads to a lower μ. Furthermore, the change in μ for contact with PC under low humidity is always greater than that for contact with NC, which is attributed to the greater temperature increase. This effect further deteriorates the electrical contact performance and tribological performance of the contact pair, potentially impacting their dynamic interaction.

3.1.3 Evolution law of the contact resistance under different humidities

Contact resistance (R_c), a critical parameter in electrical contact performance, primarily consists of contraction resistance and film resistance. Contraction resistance arises from the resistance encountered by a current as it flows through "*a* spot", as illustrated in Fig. 11. Film resistance, on the other hand, is generated by the presence of a "contaminant film" formed due to surface oxidation or external intrusion. Figure 12 presents the evolution law of the contact resistance observed in this experiment.

Figures 12(a)–12(c) illustrate the R_c under high humidity with NC and PC as the counterbody, respectively. Under identical operating parameters, the R_c in contact with the PC is significantly greater than that in contact with the NC. Additionally, R_c is negatively correlated with the normal force and current but positively correlated with the sliding speed, regardless of the humidity level.

On the basis of a series of assumptions from the Greenwood–Williamson (GW) contact model, the approximate calculation formula for contact resistance is presented in Eq. (1) [35]. As discussed in Section 3.1.2, with increasing normal force, the actual contact area of the contact surface increases, whereas the number of microbulges also increases, leading to a reduction in contact resistance. The increase in the value of parameter (a) in Eq. (1) further supports this conclusion. A comparison of the performance of the NC and PC contact pairs under both high- and low-humidity conditions, as shown in Figs. 12(a)–12(f), reveals that the PC contact surface is rougher, with a greater rough microbulge peak height and a smaller radius of curvature at the peaks. This results in a smaller actual contact area and conductive

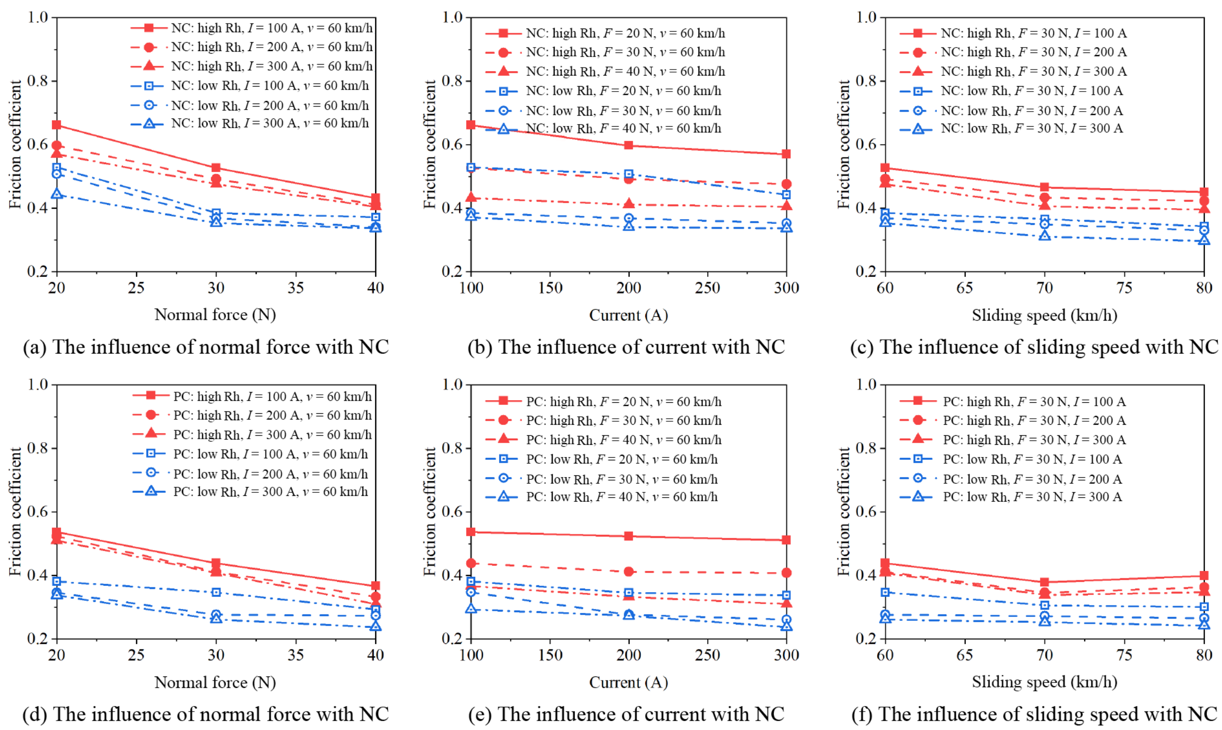

Fig. 10 Evolution law of μ with different counterbodies.

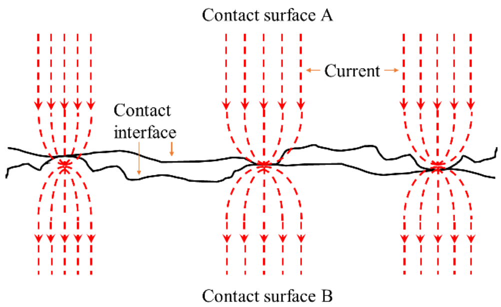

Fig. 11 Contraction resistance diagram [36].

contact area for the PC case than for the NC case (which could also be equivalent to the parameter "a" in Eq. (1)), which explains why the R_c in contact with PC is greater than that in contact with NC under identical operating conditions.

The process of current passing through the contact surfaces affects the formation of surface films and the morphology of the interface and induces heating at the contact surfaces. It also alters the structure of the regions near the surface and generates microarcing, ultimately leading to significant changes in contact resistance [2]. As the current increases, the resulting temperature increase in the contact pairs causes material softening, which reduces the peak roughness of the microbulges and increases the parameter a. Additionally, the distance between contact spots or clusters, denoted as s_{ij}, decreases. Together, these factors contribute to a reduction in R_c.

$$R_c = \frac{\rho}{\sum 2a_i} + \frac{\rho}{\pi n^2} \sum \frac{1}{s_{ij}} \tag{1}$$

where ρ is the resistivity, a is the radius of a contact spot, s is the distance between two contact spots, and n is the number of contact spot.

Figures 13(a)–13(c) illustrate the evolution law of R_c in contact with NC and PC as counterbodies under low and high humidities, respectively. Under identical operational parameters, μ under low-humidity conditions is consistently lower than that under high-humidity conditions, which aligns with previous research results [22, 23]. Additionally, parameter a increases due to the increased temperature rise under low humidity, resulting in a lower R_c.

3.2 Wear mechanism analysis of the contact strips

3.2.1 Contact strip wear mechanism for contact with PC

Previous studies have confirmed that material transfer and arcing ablation are the primary wear mechanisms for metal-impregnated carbon strips [37], regardless of humidity level [23]. However, the persistent excessive wear of strips that slide in contact with damaged contact wires necessitates further investigation into the wear mechanisms of the PCS. Although the Ref. [24] suggests that the continued increase in electrical wear of the contact strip in contact with the damaged contact wire is the main cause of the increase in the wear rate of the strip, a deeper exploration of the underlying wear submechanisms is essential for constructing wear models and understanding the mechanisms involved. Furthermore, there is still a lack of relevant research on wear mechanisms that contact damaged contact wires under low-humidity conditions.

Figures 14(a)–14(c) illustrate the microstructural morphology of the strip in contact with PC. The central area of the carbon substrate remains relatively intact under high humidity, and there are some adhesion pits and wear debris, as shown in Fig. 14(a). Focusing on Area-1, distinct thermal stress cracks are observed in the central area, which originate from localized thermal stress concentrations induced by the instantaneous high temperatures of arcing impacts. These stresses exceed the fracture strength of the material substrate, leading to crack initiation and propagation in the surrounding areas [3]. Additionally, irregular shapes resulting from solidification shrinkage cause variations in the height of the

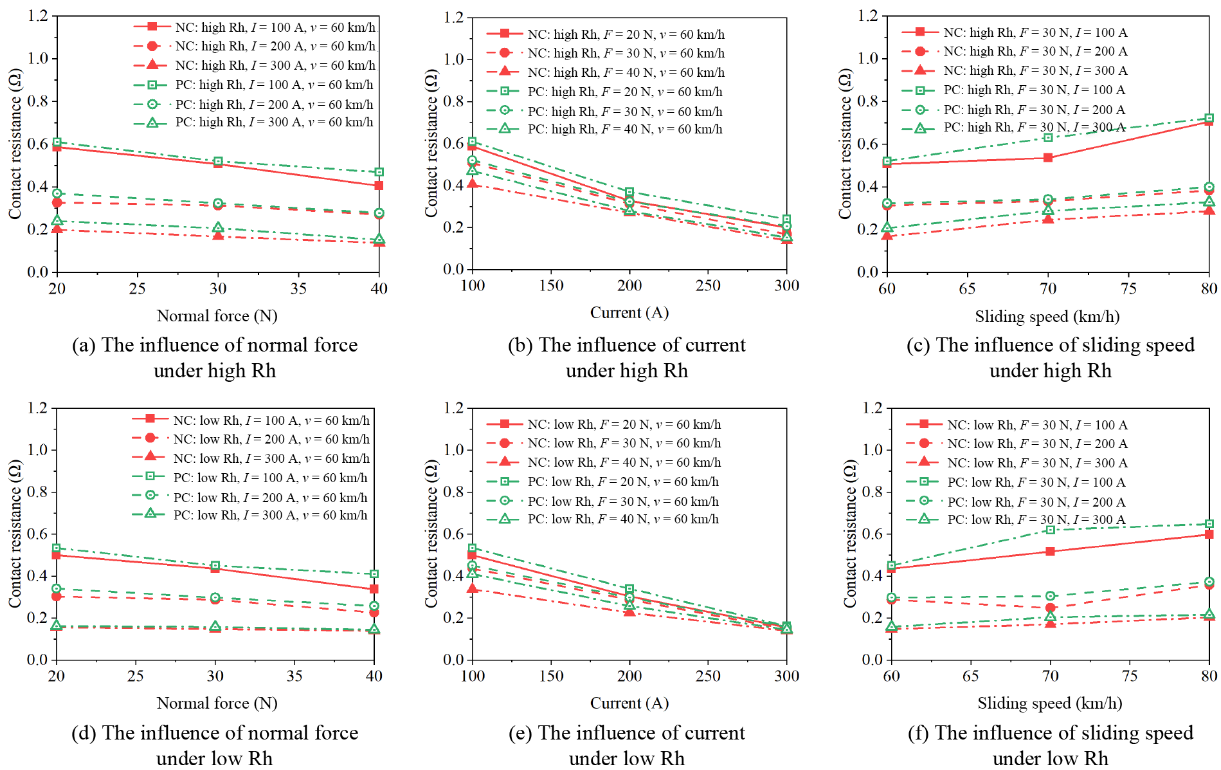

(a) The influence of normal force under high Rh
(b) The influence of current under high Rh
(c) The influence of sliding speed under high Rh
(d) The influence of normal force under low Rh
(e) The influence of current under low Rh
(f) The influence of sliding speed under low Rh

Fig. 12 Evolution law of R_c under different humidities.

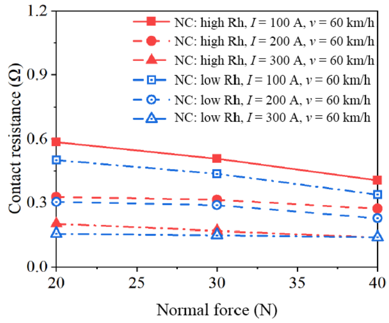

(a) The influence of normal force with NC

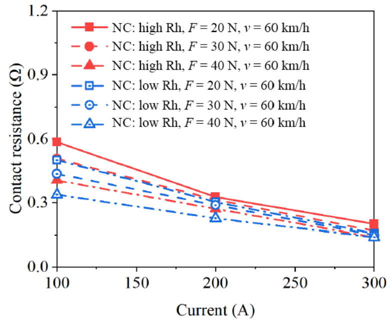

(b) The influence of current with NC

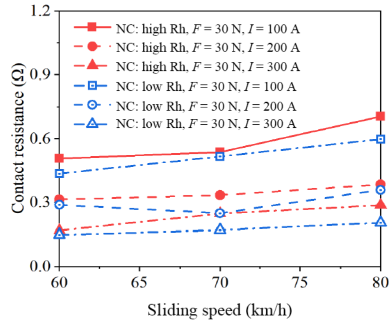

(c) The influence of sliding speed with NC

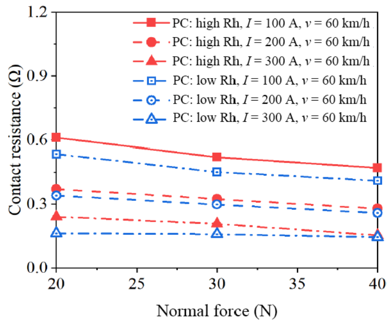

(d) The influence of normal force with NC

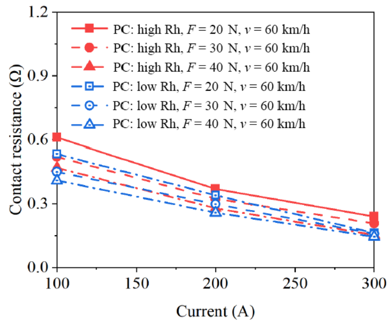

(e) The influence of current with NC

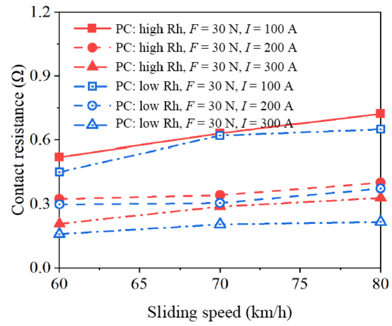

(f) The influence of sliding speed with NC

Fig. 13 Evolution law of R_c with different counterbodies.

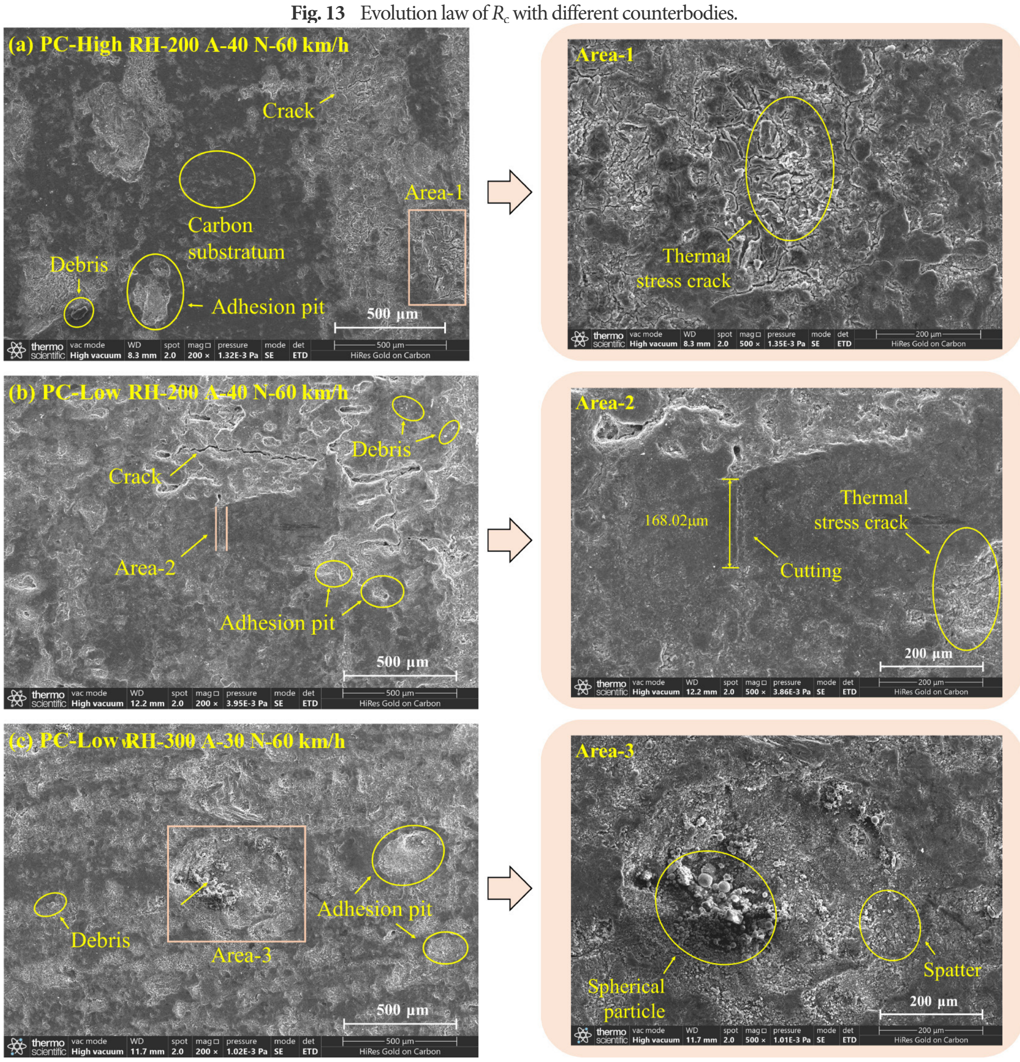

Fig. 14 Micromorphology of strip with PC counterbody.

清華大学出版社 Tsinghua University Press | SciOpen

cracks. Under the same operating conditions at low humidity, the contact surfaces also exhibit adhesion pits, wear debris, and thermal stress cracks. Notably, a microcutting length of 168.02 μm is observed, which is attributed to the deformation effects of rough contact surfaces due to damage to the carbon substrate caused by increased mechanical wear [24]. When the current is further increased to 300 A, as depicted in Fig. 13(c), severe arcing ablation marks appear on the strip surface, with a concentration of spherical particles at the ablation area, which are distinct characteristics of arcing ablation [37]. Surrounding the ablation area, numerous spatters are dispersed, contributing to the surface roughness of the strip and increasing the likelihood of abrasion, also known as mechanical wear. On the other hand, the roughness induced by arcing ablation further increases the temperature, enhancing both arcing ablation and adhesion while simultaneously increasing both electrical and mechanical wear.

Sampling of the characteristic areas on the surface of the strip revealed adhered debris and embedded spherical particles, as shown in Fig. 15. The primary elements identified include O, indicating an oxidation reaction, whereas Points 1 and 2 contain significant amounts of Cu, at 65.6% and 65.1%, respectively, far exceeding the Cu content of the substrate, suggesting that material transfer has occurred. Compared with the analysis results from NC [23], the traces of arcing ablation are more pronounced, with substantial evidence of adhesion and abrasion. Therefore, under low humidity, the primary wear mechanism involves contact with PCs under a lower current, including material transfer, arcing ablation, and microcutting, whereas at higher currents, there is an increase in material transfer and arcing ablation due to elevated Joule heating.

3.2.2 Contact strip abnormal wear mechanism in contact with a PC counterbody

To compare the severe damage caused by contact with the PC on the strip, a micromorphology analysis was conducted. Figure 16 shows the micromorphology of the strip under a normal force of 30 N, a sliding speed of 60 km/h, and currents of 200 and 300 A for both the NC and PC under high humidity. Under identical

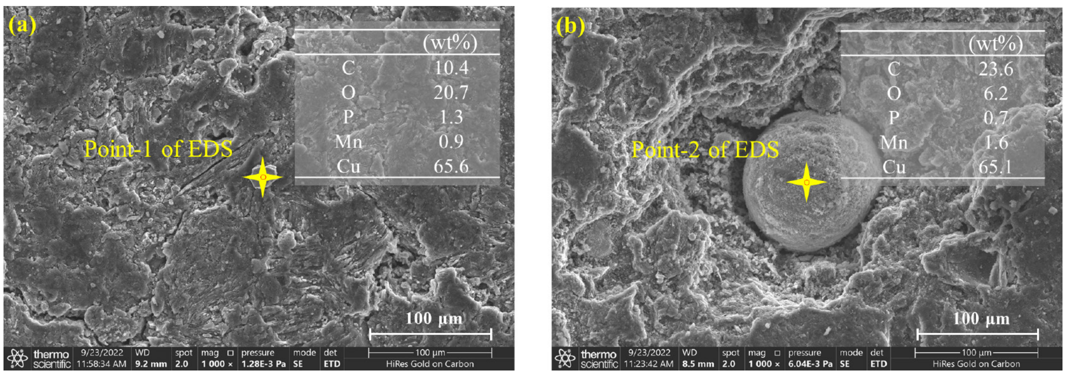

Fig. 15 EDS sample points and analysis results of strip contact with PC counterbody.

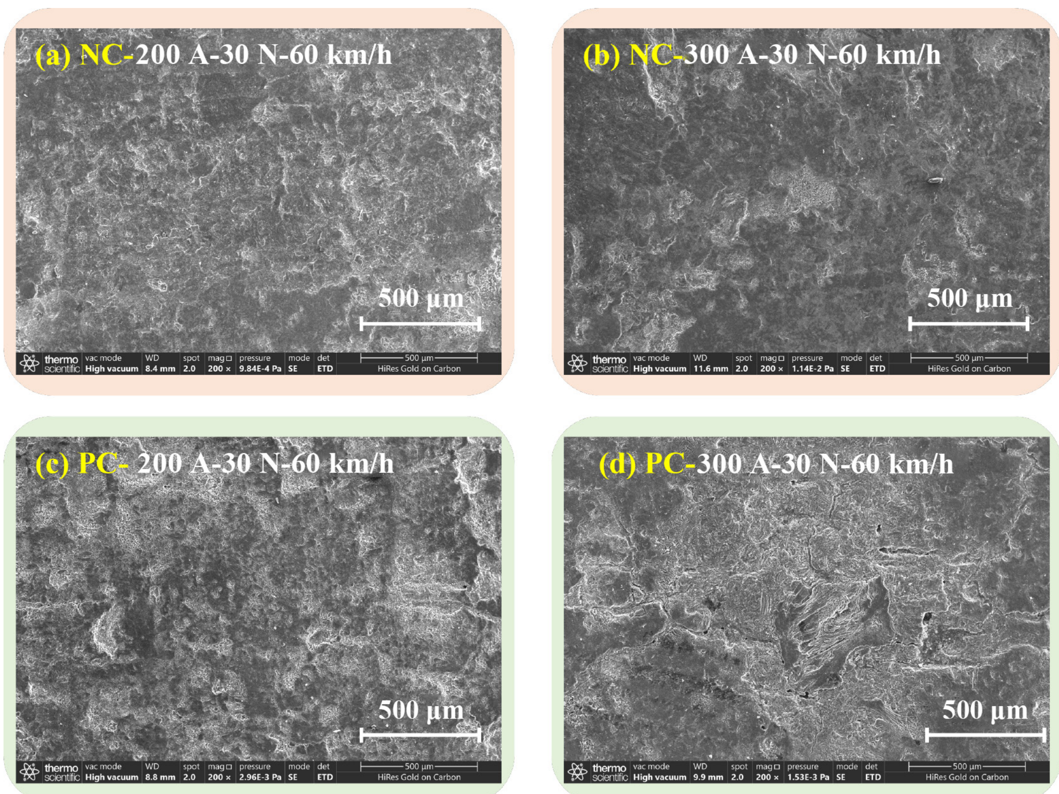

Fig. 16 Comparison of micromorphology of strips with NC and PC counterbodies.

operating conditions, the size and coverage of adhesion pits on the surface in contact with PC are greater than those in contact with NC. Furthermore, at a current of 300 A (Fig. 16(d)), a greater density of thermal stress cracks formed due to uneven thermal expansion that contacted the PC. This finding indicates that PC, when used as a counterbody, leads to more severe surface damage on the strip surface than does NC. Consequently, there is increased material transfer between the contact surfaces, as well as increased electrical and mechanical wear, resulting in greater material loss from the strip [29].

Figure 17 presents a comparison of the strip contact with PC under high and low humidities. A comparison of Fig. 17(a) with Fig. 14(b) reveals that under identical operating parameters, the strip morphology under low humidity results in more cracks, with microcutting around the cracks. The surface smoothness of the strip decreases, indicating that, compared with high humidity conditions, both electrical and mechanical wear increase under low humidity conditions. This is one of the reasons for the increased wear rate of the strip. Analysis of Figs. 17(b) and 17(c) reveals that at a current of 300 A, arcing ablation marks are nearly ubiquitous across the entire strip surface. This is because the high temperatures generated during arcing lead to the formation of oxidized material spatter, as shown in Figs. 18 and 19. O accounted for the highest proportion at 39.9%, followed by C and Cu. Furthermore, a comparison between Figs. 17(c) and 19(c) indicates that the distribution of spatter on the surface in Fig. 16(c) closely matches that of O, with a significant overlap in the distributions of O and Cu. This suggests that the spatter resulting from arcing ablation is primarily from the interaction of Cu and O. The spatter from arcing ablation adheres to the strip surface, which increases surface roughness and consequently enhances mechanical wear. Additionally, the low conductivity of copper oxide impedes current transmission, reducing the actual contact area of the microbulges that normally make contact. This can lead to the occurrence of arcing breakdown gaps, increasing the likelihood of arcing and further exacerbating both the mechanical and electrical wear of the strip. Another notable phenomenon, compared with NC, is the presence of numerous thermal stress cracks at lower currents, as shown in Fig. 17(d). This finding indicates that under low humidity conditions, when PC is used as a counterbody, uneven thermal expansion occurs at the contact surface, potentially leading to arcing discharges or other failure phenomena that cause material degradation, thereby increasing strip wear.

4 Correlation analysis of strip-influencing factors

To investigate the extent and differences in the impact of various operating parameters and wear performance parameters on strips under different counterbody and humidity conditions, this section employs a relational analysis to compare the correlation values and weights between the strip wear rate and its influencing factors. Gray relational analysis (GRA) is a multifactor statistical analysis method. If a certain indicator is known to be related to other factors, the relative strength of a project affected by the other factors can be calculated via the GRA. Specific steps include analysis sequence selection, data preprocessing, and numerical calculation [23].

Figure 20 presents the analysis results of the correlation values and weights, comparing the strips in contact with NC and PC at different humidity levels. Larger correlation values indicate a stronger correlation between each subsequence and the parent sequence, implying a more excessive influence on the parent sequence and, consequently, a more excessive impact on the wear rate. Additionally, a higher correlation weight suggests that the influencing factor has a more significant proportionate effect on the wear rate.

This section first examines the impact of different damaged

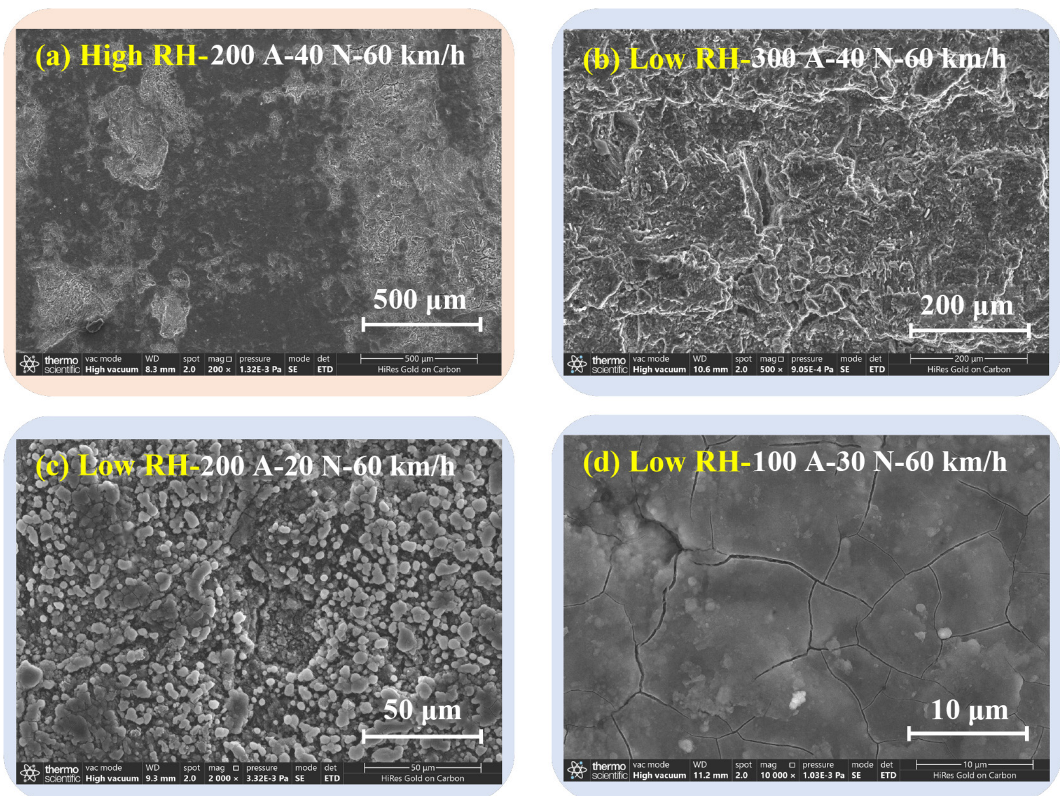

Fig. 17 Micromorphology of strip that contact with PC under different humility.

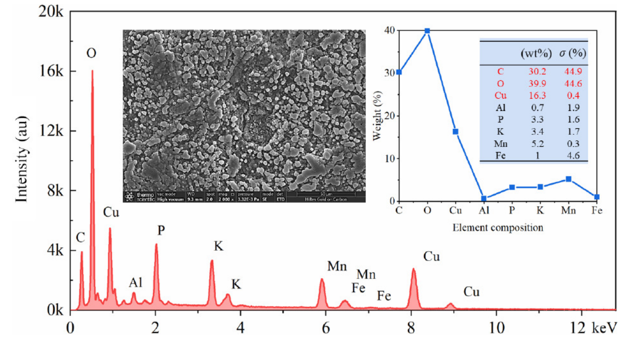

Fig. 18 EDS sample element weight analysis results of strip that contact with PC.

contact wires. The analysis results reveal that the correlation values for various parameters under PC conditions are greater than those under NC conditions, regardless of humidity level. These findings indicate that these parameters contribute more significantly to the wear rate, resulting in more excessive wear. Notably, the increase in correlation values is more pronounced under low humidity, suggesting that contact wire damage leads to more excessive wear under these conditions. In summary, both low humidity and PC conditions exacerbate wear, including both mechanical and electrical wear. Furthermore, the analysis of correlation weights indicates that after contact wire damage, the weights of the normal force, sliding speed, and friction coefficient increase, which suggests that the proportion of mechanical wear in the contact pair has increased, leading to more severe material transfer and microcutting. Additionally, the results show that, across various operating conditions, the influence of current remains the most significant, indicating that severe electrical wear is consistently present during the sliding friction process of the PCS.

With respect to the influence of humidity, the correlation values for all the parameters are greater than those under high humidity, indicating an increased contribution of these parameters to the wear rate and resulting in more excessive wear. Similarly, under low humidity, the influence weights of the normal force, sliding speed, and friction coefficient increase, leading to a greater proportion of mechanical wear during the wear process.

Figure 21 shows the differences in correlation values under various operating conditions. where ξ_{cw_1} represents the difference

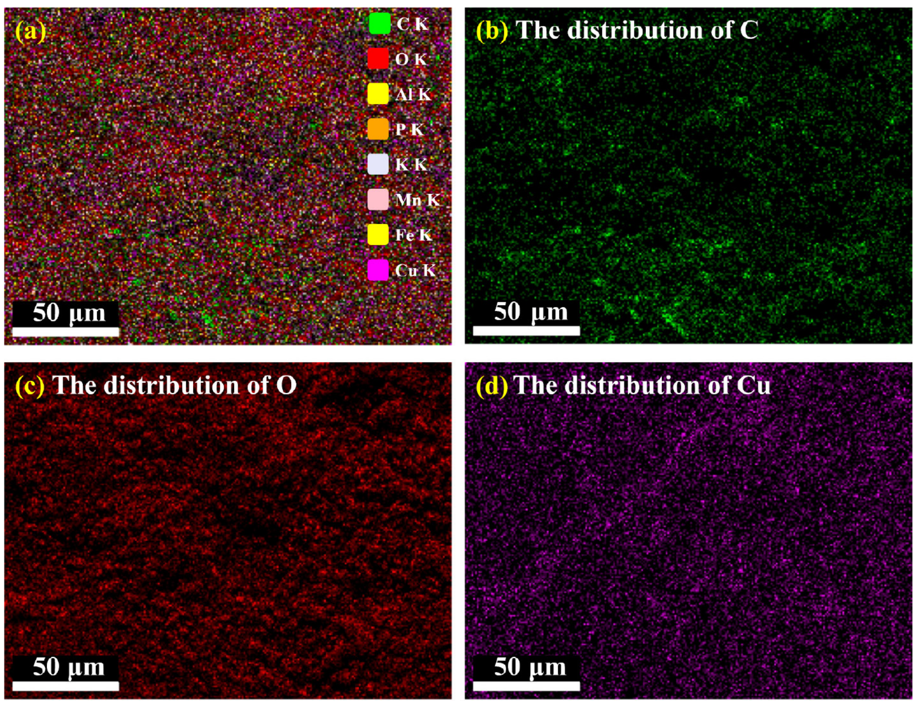

Fig. 19 EDS sample element distribution analysis results of strip that contact with PC.

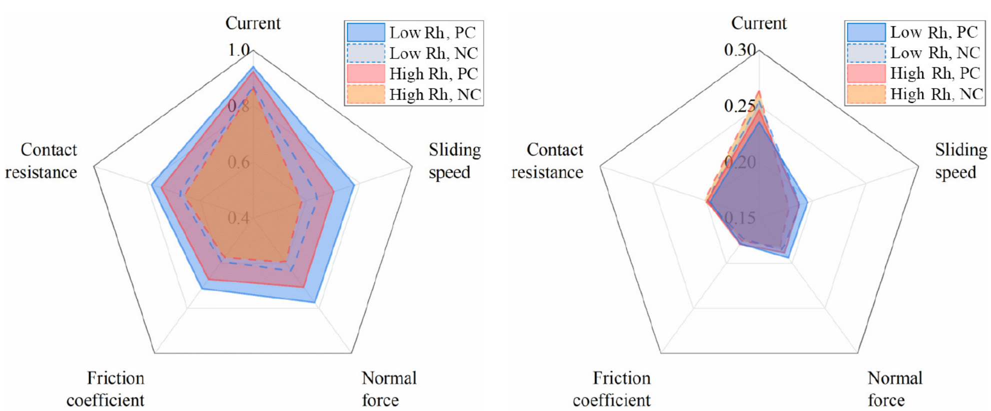

Fig. 20 Analytical results of correlation analysis.

in correlation values between PC and NC conditions under high humidity, whereas ξ_{cw_2} represents this difference under low humidity. Additionally, ξ_{Rh_1} denotes the difference in correlation values under low humidity compared with high humidity for contact with PC, and ξ_{Rh_2} represents the same contact with NC.

Based on the calculations, the following relationship is established: $\xi_{cw_2} > \xi_{cw_1} > \xi_{Rh_1} > \xi_{Rh_2}$. The smallest value is ξ_{Rh_2}, indicating that while humidity can exacerbate wear rates under normal contact wire conditions, this effect is relatively limited. Specifically, the condition $\xi_{Rh_1} > \xi_{Rh_2}$ demonstrates that when in contact with PC, low humidity significantly amplifies the impact on wear. Furthermore, the relationship $\xi_{cw_2} > \xi_{cw_1}$ suggests that low humidity exacerbates the effects of PC on wear. The highest value, ξ_{cw_2}, indicates that the wear performance of the strip is the worst when it is in contact with PC under low humidity conditions. Comparatively, ξ_{cw_i} is consistently greater than ξ_{Rh_i}, highlighting that the impact of PC on wear rates is more significant than that of humidity. In brief, the conclusion is that the worst wear performance occurs when both PC and low humidity are present simultaneously. When PC and low humidity act separately, the strip wear performance is worse with PC than with low humidity.

5 Further discussion on the causes of abnormal wear

In previous research, preliminary conclusions regarding the abnormal wear of PCSs were drawn on the basis of variations in the wear rate, μ, microstructural morphology, etc. This section integrates findings from the current study to further elucidate the causes of the continuous increase in the wear rate and to explore the underlying mechanisms of abnormal PCS wear.

The contact pair wear undergoes three stages throughout time: run-in, stability, and degradation, with the stability stage typically being the longest under normal conditions. However, the occurrence of abnormal wear significantly shortens the stability stage, potentially reducing its duration by several orders of magnitude. Understanding the wear mechanisms behind this phenomenon is complex yet crucial. Factors contributing to this include variations in operating parameters, environmental changes, degradation of structure and parameters, and deterioration of dynamic and electrical contact performance. Additionally, damage at the friction interface also plays a role. On the basis of recent field analyses, parameter matching studies, statistical data, and analyses of the wear mechanism, it has been determined that environmental factors and friction interface damage significantly contribute to abnormal wear in the PCS. This study indicates that when contact with a damaged contact wire—most notably the PC contact wire used in this work—the wear performance of the contact pair deteriorates, with more pronounced effects under low humidity. The combined impact of low humidity and PC results in different wear mechanisms of the strip. Microcutting occurs under lower current conditions, alongside material transfer and arcing ablation. As the current increases, material transfer and arcing ablation become more severe because of the deteriorating contact state. Importantly, when contact wire damage occurs, a decrease in humidity exacerbates the impact of various factors on wear performance, leading to more excessive wear.

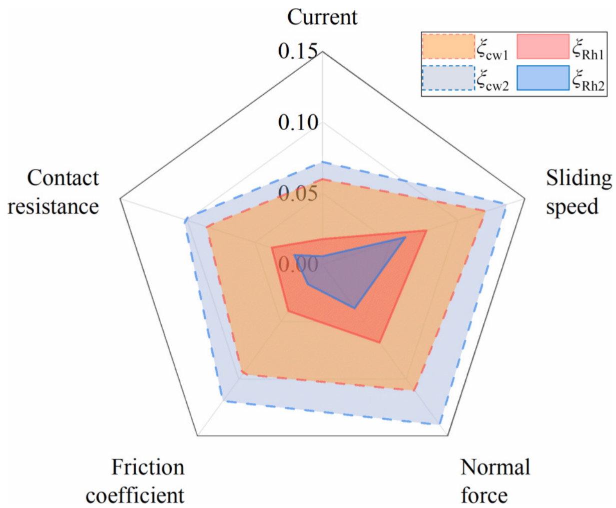

Fig. 21 Correlation value differences.

This section provides further discussion on the causes of abnormal wear. As the constant sliding friction of the contact pair, when the environmental humidity falls below a critical threshold, the contact pair surface of the PCS becomes abnormal, which can be observed both macroscopically [23] and microscopically (Figs. 14, 16, and 17), affecting both the dynamic interaction [38, 39] and wear performance. The damage to the strip is characterized primarily by the disappearance of the oxide film and uneven distribution of arcing ablation [20], as shown in Fig. 22; noticeable scratches and arcing ablation pits are evident. However, measures such as replacement or polishing can restore better current collection quality. The damage to the contact wire and its types are illustrated in Fig. 3. Considering that the contact wire can extend for tens or even hundreds of kilometers, the difficulty in locating and maintaining this damage renders it nearly irreversible. Consequently, when abnormal wear due to environmental humidity leads to contact wire damage, the situation is quite severe, and the effects of this damage surpass the reduction in humidity (Fig. 21). Although subsequent increases in humidity may occur, this irreversible damage to the contact wire continues to increase the wear rate of the strip, resulting in persistently high wear rates. If damage occurs to the contact wire while the environmental humidity remains below the critical threshold, it can inflict catastrophic damage on the contact pair, exponentially increasing both electrical and mechanical wear and leading to even more severe abnormal wear, as displayed in Condition 3 in Fig. 2. Therefore, in daily operations and maintenance, in addition to maintaining a proper temperature and humidity environment within the tunnel, urgent measures should be taken for the damaged contact wire (Fig. 3), such as polishing and reshaping. If feasible, shorter anchor sections should be installed to facilitate easier replacement of the contact wire. In addition, the next phase of work should focus on improving the identification and management of contact wire damage.

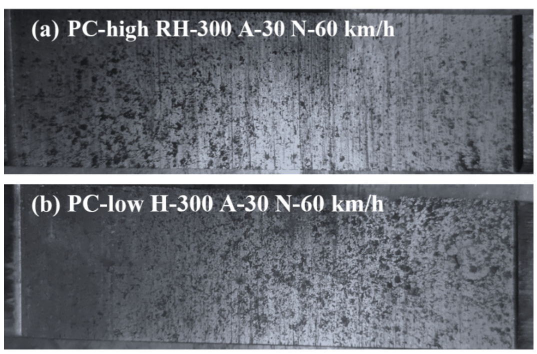

Fig. 22 Damage morphology of the strips.

6 Conclusions

In conclusion, this study investigated the wear performance of strips in contact with damaged contact wires through a series of experimental studies and data analyses conducted under both high- and low-humidity conditions. The wear mechanisms under different operating conditions were analyzed via scanning electron microscopy (SEM) and energy-dispersive X-ray spectroscopy (EDS). Finally, the correlation analysis method was employed to determine the correlation values and weights of the aforementioned tests. The specific conclusions are summarized as follows:

(1) When contact with PC, a greater amount of material transfer and arcing ablation occurs on the strip surface under high humidity than under NC. However, under low humidity conditions, when the current is relatively low, the primary wear mechanisms are material transfer, microcutting, and arcing ablation.

(2) When in contact with PC, the strip wear rate and R_c significantly increase compared with those of NC, whereas the μ decreases, both under high and low humidity. The micromorphology damage of the strip is severe, exhibiting numerous signs of arcing ablation, thermal stress cracks, and adhesion pits under low humidity, which dramatically increase both the electrical and mechanical wear of the contact pair, resulting in a 2.2-fold increase in the wear rate under the same operating parameters.

(3) Among all the influencing factors, current has the most significant impact, particularly under low humidity conditions for contact with PCs. The correlation value for contact with PC is noticeably greater than that for contact with NC. Similarly, the correlation value under low humidity conditions is greater than that under high humidity, which both cause excessive wear on the strip and result in an increased proportion of mechanical wear. ξ_{cw_i} is consistently greater than ξ_{Rh_i}, indicating that contact wire damage has a more pronounced effect on the wear rate than does humidity. Therefore, it is essential to implement corrective measures promptly after any contact wire damage to mitigate wear.

(4) When the humidity falls below the critical threshold, the contact state of the friction pair becomes abnormal, leading to surface damage that deteriorates the dynamic interaction and wear performance of the PCS. This results in severe mechanical wear and electrical degradation, causing abnormal wear and a dramatic increase in the wear rate.

Acknowledgements

This research was supported by the National Natural Science Foundation of China (No. U2469213), the National Key R&D Program of China (No. 2022YFB4301201-03), and the Independent Project of State Key Laboratory of Rail Transit Vehicle System (Nos. 2023TPL-T05 and 2024RVL-T05).

Declaration of competing interest

The authors have no competing interests to declare that are relevant to the content of this article.

References

[1] Zhang W H. *Dynamics of Coupled Systems in High-Speed Railways*. Elsevier Inc., 2020.

[2] Fischer A, Dudziński W, Gleising B, Stemmer P. Analyzing mild- and ultra-mild sliding wear of metallic materials by transmission electron microscopy. Dienwiebel M, de Barros Bouchet M I, Eds. In: *Advanced Analytical Methods in Tribology*. Berlin: Springer Cham, 2018: 29–59.

[3] Braunovic M, Myshkin N K, Konchits V V. *Electrical Contacts: Fundamentals, Applications and Technology*. Florida (USA): CRC Press, 2017.

[4] Czichos H. Tribology: A systems approach to the Science and Technology of friction, lubrication and wear. *Tribol Int* **100**(4): 513–514 (1978)

[5] Kar S, Bandyopadhyay P P, Paul S. Effect of arc–current and spray distance on elastic modulus and fracture toughness of plasma-sprayed chromium oxide coatings. *Friction* **6**(4): 387–394 (2018)

[6] Braceras I, Ibáñez I, Dominguez-Meister S, Velasco X, Brizuela M, Garmendia I. Electro-tribological properties of diamond like carbon coatings. *Friction* **8**(2): 451–461 (2020)

[7] Wang R, Zhang Z, Zhong J. Analysis and research on current-carrying friction and wear of high-speed train pantograph slide and contact wire based on computer simulation analysis. *J Phys Conf Ser* **1648**(3): 032031 (2020)

[8] Zhao J, Peng Y T, Zhou Q G, Zou K. The current-carrying tribological properties of Cu/graphene composites. *J Tribol* **143**(10): 102101 (2021)

[9] Wang P, Wei F C, Zhao Z W, Guo Y G, Du S M, Hao Z H. Effect of heat treatment temperature on mechanical and tribological properties of copper impregnated carbon/carbon composite. *Tribol Int* **164**: 107209 (2021)

[10] Ding T, Chen G X, Zhu M H, Zhang W H, Zhou Z R. Influence of the spring stiffness on friction and wear behaviours of stainless steel/copper-impregnated metallized carbon couple with electrical current. *Wear* **267**(5–8): 1080–1086 (2009)

[11] Wang J P, Ren C L, Hong L. The construction parameter optimization of high-speed pantograph. *J Phys Conf Ser* **2025**(1): 012094 (2021)

[12] Song Y, Rønnquist A, Jiang T J, Nåvik P. Identification of short-wavelength contact wire irregularities in electrified railway pantograph-catenary system. *Mech Mach Theory* **162**: 104338 (2021)

[13] Wu Y L, Fu W M, Huang H, Chen G X, Gao G Q, Wu G N. Effect of the staggering on the wear performance of carbon strip/Cu–Ag alloy contact wire with electric current. *Lubr Eng* **42**(10): 57–61 (2017) (in Chinese)

[14] Yang H J, Hu B, Liu Y H, Cui X L, Jiang G. Influence of reciprocating distance on the delamination wear of the carbon strip in pantograph-catenary system at high sliding-speed with strong electrical current. *Eng Fail Anal* **104**: 887–897 (2019)

[15] Liew W Y H. Effect of relative humidity on the unlubricated wear of metals. *Wear* **260**(7–8): 720–727 (2006)

[16] Czyzniewski A. The effect of air humidity on tribological behaviours of W–C: H coatings with different tungsten contents sliding against bearing steel. *Wear* **296**(1–2): 547–557 (2012)

[17] Helmick L S, Sharma S K. Effect of humidity on wear of M-50 steel with a branched perfluoropolyalkylether lubricant. *Tribol Lett* **6**(2): 123–127 (1999)

[18] Wang X, Wang P, Zhang B, Yang S R, Zhang J Y. The tribological properties of fullerene-like hydrogenated carbon (FL–C: H) film under different humidity conditions. *Tribol T* **52**(3): 354–359 (2009)

[19] Moberly L E, Johnson J L. Wear and friction of carbon brushes as a functionof air humidity. In: Proceedings of the 4th Conference on Carbon, 1959: 711–718.

[20] Hu Z L, Chen Z H, Xia J T. Study on surface film in the wear of electrographite brushes against copper commutators for variable current and humidity. *Wear* **264**(1–2): 11–17 (2008)

[21] Wu R X, Song C F, Wu H H, Lv B, Zhang Y Y, Zhang Y Z. Effect of relative humidity on the current-carrying tribological properties of Cu–C sliding contact pairs. *Wear* **492**: 204219 (2022)

[22] Song C F, Sun Y X, Zhang Y Y, Pang X J, Chen T H, Sun C, Zhang Y Z. Current-carrying property and damage mechanism of rolling

contact pairs in different water conditions: From vapor to liquid. *Wear* **477**: 203857 (2021)
[23] Zhi X S, Zhou N, Cheng Y, Wang X Y, Wei H F, Chen G X, Zhang W H. Effect and behaviors of ambient humidity on the wear of metal-impregnated carbon strip in pantograph-catenary system. *Tribol Int* **188**: 108864 (2023)
[24] Ren W J, Chen G X, Dong B J, Song Q F, Feng X H, Li L, Yang H J, He Q X. Experimental study of the effect of contact line profiles on the wear mechanism of a skateboard. *Tribol Int* **192**: 109317 (2024)
[25] Bouchoucha A, Chekroud S, Paulmier D. Influence of the electrical sliding speed on friction and wear processes in an electrical contact copper–stainless steel. *Appl Surf Sci* **223**(4): 330–342 (2004)
[26] Lin X Z, Zhu M H, Mo J L, Chen G X, Jin X S, Zhou Z R. Tribological and electric-arc behaviors of carbon/copper pair during sliding friction process with electric current applied. *T Nonferr Metal Soc* **21** (2): 292–299 (2011)
[27] Yang H J, Chen G X, Gao G Q, Wu G N, Zhang W H. Experimental research on the friction and wear properties of a contact strip of a pantograph-catenary system at the sliding speed of 350 km/h with electric current. *Wear* **332**: 949–955 (2015)
[28] Collina A, Melzi S, Facchinetti A. On the prediction of wear of contact wire in OHE lines: A proposed model. *Vehicle Syst Dyn* **37** (sup1): 579–592 (2002)
[29] Bucca G, Collina A. A procedure for the wear prediction of collector strip and contact wire in pantograph-catenary system. *Wear* **266**(1–2): 46–59 (2009)
[30] Wei X K, Meng H F, He J H, Jia L M, Li Z G. Wear analysis and prediction of rigid catenary contact wire and pantograph strip for railway system. *Wear* **442**: 203118 (2020)
[31] Zhou N, Zhi X S, Cheng Y, Sun Y, Wang J L, Gu Z L, Li Z Y, Zhang W H. Contact strip of pantograph heuristic wear model and its application. *Tribol Int* **194**: 109546 (2024)
[32] Mishina H, Hase A. Effect of the adhesion force on the equation of adhesive wear and the generation process of wear elements in adhesive wear of metals. *Wear* **432**: 202936 (2019)
[33] Simarro M, Postigo S, Casanueva C, Rodríguez-Tembleque L, Castillo J J. Influence of main operating conditions on contact wire wear of rigid catenary lines. *Tribol Int* **196**: 109708 (2024)
[34] Markov D P. Adhesion at friction and wear. *Friction* **10**(11): 1859–1878 (2022)
[35] Greenwood J A. Constriction resistance and the real area of contact. *Brit J Appl Phys* **17**(12): 1621–1632 (1966)
[36] Holm R. *Electric Contacts: Theory and Application*. Berlin (Germany): Springer, 1967.
[37] Wu G N, Zhou Y, Gao G Q, Wu J, Wei W F. Arc erosion characteristics of Cu-impregnated carbon materials used for current collection in high-speed railways. *IEEE T Compon Pack T* **8**(6): 1014–1023 (2018).
[38] Mirzababaei S, Filip P. Impact of humidity on wear of automotive friction materials. *Wear* **376**: 717–726 (2017)
[39] Yao Y M, Zhou N, Mei G M, Zhang W H. Dynamic analysis of pantograph-catenary system considering ice coating. *Shock Vib* **2020** (1): 8887609 (2020).

Xingshuai Zhi received his master degree in State Key Laboratory of Rail Transit Vehicle system, Southwest Jiaotong University, China, in 2023. Now, he is a Ph.D. student at State Key Laboratory of Rail Transit Vehicle system, Southwest Jiaotong University, China. His research interests include current-carrying friction and wear, tribo-dynamics.

Ning Zhou received his M.S. degree in Xi'an Jiaotong University, China, in 2000. He received his Ph.D. degree in State Key Laboratory of Rail Transit Vehicle system, Southwest Jiaotong University, China, in 2013. His current position is a professor at Southwest Jiaotong University, China. His research interests include vehicle system dynamics, tribology/dynamic behavior analysis.

Yao Cheng received his M.S. and Ph.D. degrees in State Key Laboratory of Rail Transit Vehicle system, Southwest Jiaotong University, China, in 2013 and 2019, respectively. His current position is an assistant professor at Southwest Jiaotong University, China. His research interests include the theory and application of high-speed train on-line monitoring and fault diagnosis.

Haifei Wei received his master degree in State Key Laboratory of Rail Transit Vehicle system, Southwest Jiaotong University, China, in 2023. Now, he is a Ph.D. student at State Key Laboratory of Rail Transit Vehicle system, Southwest Jiaotong University, China. His research interests include structural damage analysis, tribo-dynamics.

Yongming Yao received his Ph.D. degree in vehicle engineering from Southwest Jiaotong University, Chengdu, China, in 2021. He is currently a research associate in the Power Supply Inspection Research Department of the Infrastructure Inspection Research Institute of China Academy of Railway Sciences Group Co., Ltd. His current research interests are pantograph-catenary dynamics, catenary detection, catenary fault diagnosis and machine learning.

Weihua Zhang received his M.S. and Ph.D. degrees in Southwest Jiaotong University, China, in 1989 and 1996, respectively. His current position is a distinguished professor at Southwest Jiaotong University, China. His research interests include vehicle system dynamics, tribology/dynamic behavior analysis.

Guangxiong Chen received his M.S. and Ph.D. degrees in Department of Mechanical Engineering, Southwest Jiaotong University, China, in 1988 and 2002, respectively. His current position is a professor at Tribology Research Institute of Southwest Jiaotong University, China. His research interests include tribology/dynamic behavior analysis, vibration, and noise control.